

See discussions, stats, and author profiles for this publication at: <https://www.researchgate.net/publication/224895078>

# Photocatalytic Activities of Different Well-defined Single Crystal TiO<sub>2</sub> Surfaces: Anatase versus Rutile

ARTICLE *in* JOURNAL OF PHYSICAL CHEMISTRY LETTERS · OCTOBER 2011

Impact Factor: 7.46 · DOI: 10.1021/jz201156b

---

CITATIONS

53

---

READS

118

## 4 AUTHORS, INCLUDING:



**Amira Ahmed**

Sohag University

5 PUBLICATIONS 65 CITATIONS

SEE PROFILE



**Tarek A. Kandiel**

Faculty of Science, Sohag University

22 PUBLICATIONS 551 CITATIONS

SEE PROFILE



**Torsten Oekermann**

Friemann & Wolf Batterietechnik GmbH

65 PUBLICATIONS 1,728 CITATIONS

SEE PROFILE

# Photocatalytic Activities of Different Well-defined Single Crystal TiO<sub>2</sub> Surfaces: Anatase versus Rutile

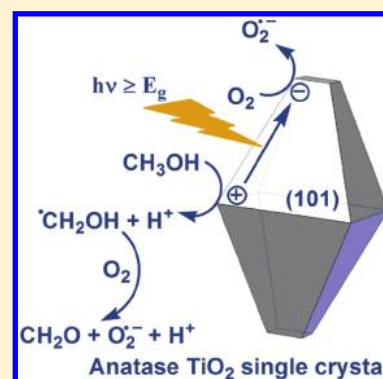
Amira Y. Ahmed,<sup>†,§</sup> Tarek A. Kandiel,<sup>†,§</sup> Torsten Oekermann,<sup>†,⊥</sup> and Detlef Bahnemann<sup>\*,†</sup>

<sup>†</sup>Institute of Physical Chemistry and Electrochemistry and <sup>‡</sup>Institute of Technical Chemistry, Leibniz Universität Hannover, Callinstrasse 3A, 30167 Hannover, Germany

<sup>§</sup>Department of Chemistry, Faculty of Science, Sohag University, Sohag 82524, Egypt

**ABSTRACT:** The photocatalytic activities of well-defined TiO<sub>2</sub> single-crystal anatase (101) surfaces have been assessed by methanol oxidation and by terephthalic acid hydroxylation evincing the formation of OH• radicals and have been compared with that of rutile single-crystal (001), (100), and (110) surfaces. The results showed that the anatase (101) surface exhibits a higher photocatalytic activity than all investigated rutile surfaces toward the oxidation of methanol and exhibits a comparable activity to that of the rutile (001) surface with respect of terephthalic acid hydroxylation. The rutile (001) surface shows a higher photocatalytic activity than both the rutile (110) and (100) surfaces for both photocatalytic test reactions. Because anatase (101) and rutile (110) are the thermodynamically most stable surfaces, anatase and rutile nanomaterials possess, thus, a large percentage of (101) and (110) surfaces, respectively. This offers a reasonable explanation why anatase nanoparticles usually exhibit higher photocatalytic activities than the respective rutile powders.

**SECTION:** Surfaces, Interfaces, Catalysis



Owing to the scientific and technological importance of titanium dioxide (TiO<sub>2</sub>) photocatalysts, much effort has been devoted to the understanding of the photocatalytic processes occurring at its surface.<sup>1</sup> Almost all of the studies that have so far been carried out using photoelectrochemical measurements employing the thermodynamically most stable polymorph, that is, the rutile (110) surface mainly due to its commercial availability. In contrast, hardly any photocatalytic experiments on well-defined anatase surfaces have so far been reported.<sup>2</sup> However, technical-grade TiO<sub>2</sub> is very often supplied in the anatase form; most TiO<sub>2</sub> nanomaterials are produced in the anatase form, and in most cases, anatase is reported to be photocatalytically more active than rutile.<sup>3</sup> This lack of experimental data on anatase single-crystal surfaces is mostly due to the limited availability of anatase crystals of sufficiently large size.<sup>4,5</sup> This has motivated several theoretical investigations of anatase,<sup>6–9</sup> but there clearly is lack of experimental data in the literature obtained on well-defined anatase surfaces that could enable verification of these theoretical predictions.

During the past decades, most photocatalytic studies employing TiO<sub>2</sub> nanomaterials indicate that their photocatalytic activity for the decomposition of organic molecules is an extremely complex matter and appears to depend strongly on both the model substrate and the physical properties of TiO<sub>2</sub> particles.<sup>3,10–13</sup> In general, anatase nanomaterials display photocatalytic activities that are higher than those of rutile;<sup>3</sup> however, in some cases, the latter has shown better activities than the former.<sup>14</sup> Research to examine the surprising

differences in photocatalytic activity between anatase and rutile has so far focused almost exclusively on the comparison of the powdered forms of these two TiO<sub>2</sub> modifications. These studies are important, but by their nature, the powdered forms of TiO<sub>2</sub> are poorly defined, and it is thus almost impossible to draw any conclusive scientific concepts concerning the photocatalytic activities of TiO<sub>2</sub> photocatalysts from this work.

One of the most serious experimental problems is the difficulty encountered in the preparation of TiO<sub>2</sub> photocatalysts exhibiting the same physical and optical properties, that is, identical surface area, particle size, exposed surface, band gap energy and position, crystallinity, morphology, and light absorption capability, to name but a few. A limited number of studies have suggested a significant role of the exposed surface of TiO<sub>2</sub> polyhedral particles on their photocatalytic activity.<sup>13,15</sup> Thus, there appears to be an urgent need to examine the photocatalytic activities of different well-defined TiO<sub>2</sub> surfaces. In contrast to TiO<sub>2</sub> nanomaterials, where the comparison of the powdered forms of these two modifications has so far not resulted in any reliable database and hence many hypotheses have been proposed, these well-defined surfaces provide a reliable basis for the direct comparison between the photocatalytic activities of anatase and rutile.

**Received:** August 24, 2011

**Accepted:** September 14, 2011

**Published:** September 16, 2011

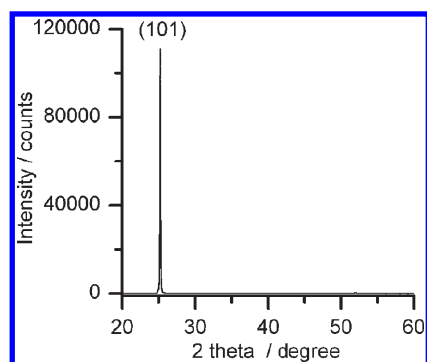


**Figure 1.** XRD diffraction pattern of the anatase  $\text{TiO}_2$  single-crystal surface.

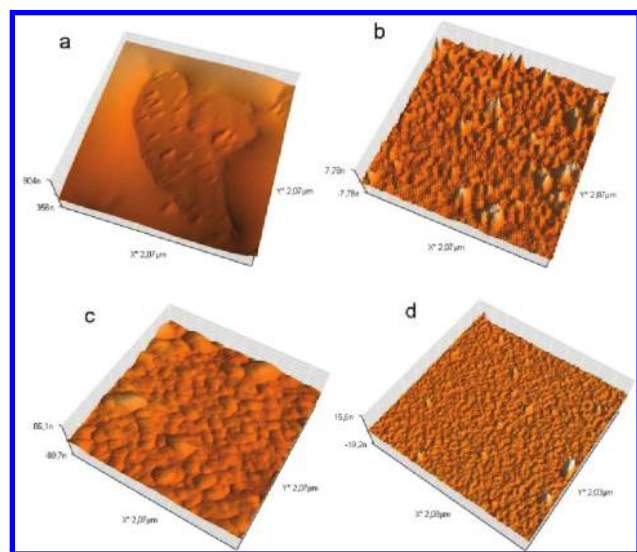


**Figure 2.** Three-dimensional AFM images of (a) the anatase  $\text{TiO}_2$  single-crystal (101) surface and (b–d) the rutile  $\text{TiO}_2$  single-crystal (001), (100), and (110) surfaces, respectively.

Because it is usually rather difficult to prepare anatase single crystals in the laboratory, the anatase (101) surfaces employed in the present study have been obtained from a natural mineral single crystal that has been oriented, cleaved, and polished. The resulting surface was  $3 \times 3 \times 0.5 \text{ mm}^3$  in size. It was initially clear with an orange shade and turned gray after exposure to a stream of hydrogen gas at  $600^\circ\text{C}$  for 2 h to achieve n-type doping by oxygen vacancies. Rutile  $\text{TiO}_2$  single-crystal surfaces with a size of  $10 \times 10 \times 0.5 \text{ mm}^3$  exhibiting a polished (110), (001), or (001) surface, respectively, on one side were purchased from K & R Creation Co., Japan, and cut into pieces of  $5 \times 5 \times 0.5 \text{ mm}^3$ . To achieve n-type doping by oxygen vacancies, the wafers were also exposed to a stream of hydrogen gas, employing the same experimental conditions as in the case of the anatase (101) surface.

The anatase (101) surface and the rutile (001), (100), and (110) surfaces have been characterized by X-ray diffraction (XRD) and by atomic force microscopy (AFM). Figure 1 shows the XRD pattern of  $\text{TiO}_2$  anatase (101). It is obvious from the high intensity of the XRD pattern that the anatase single crystal is of high quality, exhibiting a perfect (101) surface. No other reflections have been observed, revealing the perfect

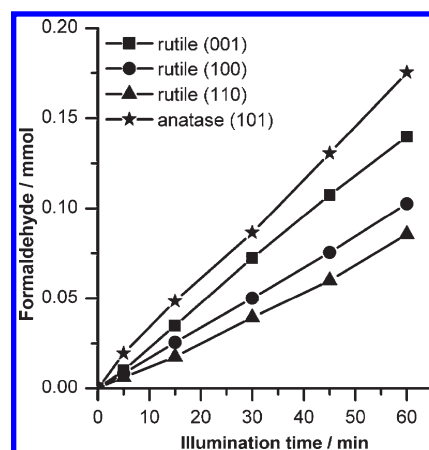


**Figure 3.** Photocatalytic methanol oxidation to formaldehyde on different  $\text{TiO}_2$  single-crystal surfaces under  $35 \text{ mW}/\text{cm}^2$  UV(A) illumination as a function of time; the illuminated area of rutile and anatase surfaces are  $0.25$  and  $0.09 \text{ cm}^2$ , respectively. Note: the amount of formaldehyde formed on the anatase surface has been normalized to  $0.25 \text{ cm}^2$ .

cutting parallel to the (101) direction. Figure 2 shows the three-dimensional AFM images for the  $\text{TiO}_2$  anatase (101) and the rutile (001), (100), and (110) surfaces. It can clearly be seen that all surfaces exhibit a relatively rough texture.

The photocatalytic activities of the different  $\text{TiO}_2$  single-crystal surfaces have been assessed by the photocatalytic oxidation of methanol. Methanol has been chosen as a model compound because it has been shown to be a suitable molecular probe to explore surface properties through different experimental techniques.<sup>16,17</sup> Moreover, methanol has been frequently used as a hole scavenger to achieve enhanced photocatalytic hydrogen production rates.<sup>18,19</sup> The photocatalytic experiments have been carried out employing  $3.5 \text{ mL}$  standard rectangular quartz cuvettes. For easier handling of the single-crystal surfaces, they have been fixed by connecting copper wires to the surfaces opposite to the polished surfaces of these single-crystal surfaces using conductive epoxy resin. The copper wires were covered with glass tubes, and the connections between the glass tubes and the wafers, except for the polished surfaces, were sealed with nonconductive epoxy resin (Araldite Rapid, Ciba Geigy). Afterward, the single-crystal surfaces were immersed in  $3 \text{ mL}$  of  $1 \text{ vol } \%$  aerated methanol aqueous solutions and illuminated by UV(A) light filtered through a  $320 \text{ nm}$  long-pass cutoff filter (LOT-Oriel, Germany, light intensity  $35 \text{ mW cm}^{-2}$ ) for different times using a high-pressure Xe lamp (OSRAM HBO 450 W). Methanol was photocatalytically oxidized to formaldehyde. The produced formaldehyde was analyzed by employing HPLC using the Nash reagent.<sup>20</sup> Figure 3 shows the time course of formaldehyde formation on the different  $\text{TiO}_2$  single-crystal surfaces. It is obvious from the results shown in Figure 3 that the anatase (101) surface exhibits a higher photocatalytic activity than any of the investigated rutile surfaces.

Because the photocatalytic tests have been carried out by employing aqueous methanol solutions, there will be a competition between the direct photo-oxidation of methanol and that of water on the  $\text{TiO}_2$  surfaces. It remains unclear whether the methanol photo-oxidation proceeds via the direct interfacial transfer of photogenerated holes or involves the reaction with photogenerated hydroxyl radicals ( $\text{OH}^\bullet$ ) as an intermediate step.<sup>21,22</sup> It is a frequently employed concept that hydroxyl

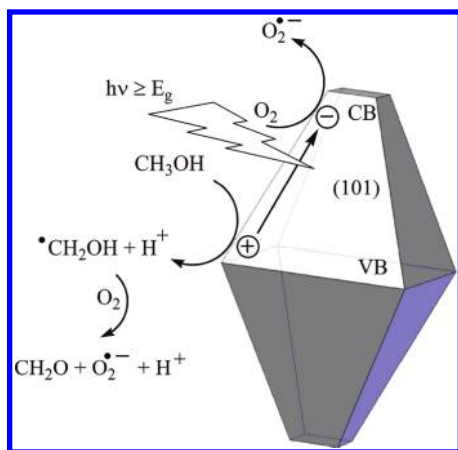


**Figure 4.** Scheme representing the photocatalytic steps of methanol photo-oxidation on the anatase  $\text{TiO}_2$  single-crystal (101) surface. Note: for simplicity, the formation of hydroxymethyl radicals ( $\text{*CH}_2\text{OH}$ ) by  $\text{OH}^\bullet$  radicals is represented by the hole oxidation step.

radical species are responsible for the oxidation pathways of chemical compounds initiated by heterogeneous photocatalytic processes. For instance, methanol has been employed as a  $\text{OH}^\bullet$  radical scavenger in order to determine the quantum yield and photonic efficiency of  $\text{OH}^\bullet$  radical generation from photogenerated holes at the  $\text{TiO}_2$  surface.<sup>22–24</sup> Methanol reacts with  $\text{OH}^\bullet$  radicals and/or with surface-trapped holes, leading to the formation of  $\text{*CH}_2\text{OH}$  radicals. The latter is further oxidized by reacting with molecular oxygen, leading to the formation of formaldehyde. The possible reaction steps are illustrated in Figure 4.

The photonic efficiencies ( $\zeta$ ) of the methanol photo-oxidation on the different  $\text{TiO}_2$  single-crystal surfaces have been calculated by dividing the rate of formaldehyde formation ( $r$ ) by the incident photon flux ( $I_0$ ) according to the following equation<sup>25</sup>

$$\zeta = r \times 100 / I_0$$

The incident photon flux per  $0.25 \text{ cm}^2$  of illuminated surface has been calculated to be  $1.54 \mu\text{Einstein min}^{-1}$  based on the UV(A) light meter measurements and assuming an average illumination wavelength of  $\lambda = 350 \text{ nm}$ . The rates of formaldehyde formation ( $\mu\text{mol min}^{-1}$  per  $0.25 \text{ cm}^2$  of electrode surface area) have been calculated from the slope of the time course of formaldehyde formation presented in Figure 3. The photonic efficiency of the anatase (101) surface has been calculated to be  $\zeta = 0.190\%$ , while the photonic efficiencies of the rutile (001), (100), and (110) surfaces have been calculated to be  $\zeta = 0.153$ ,  $0.110$ , and  $0.089\%$ , respectively. The photonic efficiency values of all well-defined  $\text{TiO}_2$  surfaces investigated here are higher than the reported value ( $\zeta = 0.036$ )<sup>26</sup> for methanol photo-oxidation on nanocrystalline  $\text{TiO}_2$  layers and also higher than the reported values for methylene blue photodegradation on anatase and on Pilkington active films,<sup>27</sup> evincing that the tuning of the exposed surface should be able to further enhance the photocatalytic activity of  $\text{TiO}_2$  coatings.

The photocatalytic activities of the anatase and the different rutile single-crystal surfaces have also been evaluated by the photocatalytic hydroxylation of terephthalic acid, which is usually regarded as an indirect detection of  $\text{OH}^\bullet$  radicals. Therefore, the  $\text{OH}^\bullet$  radical formation at the  $\text{TiO}_2$  surfaces has been detected by

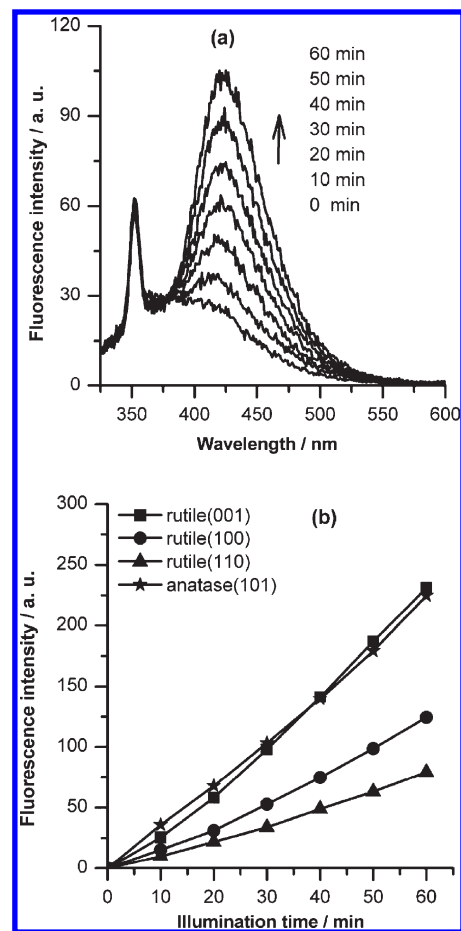


**Figure 5.** (a) Fluorescence spectra of a  $4 \times 10^{-4} \text{ M}$  basic solution of terephthalic acid excited at  $315 \text{ nm}$  as a function of illumination time; the illuminated area of anatase surface is  $0.09 \text{ cm}^2$ . (b) Fluorescence intensity at  $425 \text{ nm}$  as a function of illumination time; the illuminated areas of the rutile and anatase surfaces are  $0.25$  and  $0.09 \text{ cm}^2$ , respectively. Note: the fluorescence intensity on the anatase surface has been normalized to  $0.25 \text{ cm}^2$ .

measuring the fluorescence intensity at  $425 \text{ nm}$  of 2-hydroxyterephthalic acid excited by  $315 \text{ nm}$ . The single-crystal surfaces have been immersed in standard rectangular quartz cuvettes containing  $2 \text{ mL}$  of a  $4 \times 10^{-4} \text{ M}$  basic solution of terephthalic acid and have been illuminated by UV(A) light filtered through a  $320 \text{ nm}$  long-pass cutoff filter (LOT-Oriel, Germany, light intensity  $15 \text{ mW cm}^{-2}$ ) for different times using a high-pressure Xe lamp (OSRAM HBO 450 W). Terephthalic acid reacts with the  $\text{OH}^\bullet$  radicals, leading to formation of 2-hydroxyterephthalic acid.<sup>28</sup> Figure 5a shows the change in the fluorescence spectra recorded for the terephthalic acid solution under UV illumination in the presence of the anatase (101) surface (shown as an example). Figure 5b shows the change in fluorescence intensity recorded for the basic terephthalic acid solution under UV(A) illumination as a function of irradiation time for the anatase (101) surface and for the rutile (001), (100), and (110) surfaces, respectively. The linear relationship between the fluorescence intensity and irradiation time indicates that the amount of  $\text{OH}^\bullet$  generated on the  $\text{TiO}_2$  surface is proportional to the irradiation time during the photocatalytic process. Figure 5b clearly shows that the rate of  $\text{OH}^\bullet$  radical formation on the anatase (101) surface is comparable to that on the rutile (001) surface and higher than that on the



rutile (100) and (110) surfaces. This trend is the same as that observed for the photocatalytic oxidation of methanol, except that anatase (101) and rutile (001) exhibit more or less the same photocatalytic activities toward  $\text{OH}^\bullet$  generation. The higher activity of the photocatalytic methanol oxidation on the anatase (101) surface as compared with that on the rutile (001) surface, despite the fact that both of them show the same  $\text{OH}^\bullet$  radical generation activity, can be explained either by direct interfacial transfer of photogenerated holes leading to the photocatalytic oxidation of methanol or by the fact that the photogenerated  $\text{OH}^\bullet$  radicals on the anatase (101) surface are more reactive than those on the rutile (001) surface at least toward methanol photo-oxidation.

The reduced reactivity of  $\text{OH}^\bullet$  radical generation on the rutile (110) surface in comparison to that on the anatase (101) surface is in agreement with the behavior observed on rutile and anatase powders reported by Hirakawa et al.<sup>29</sup> For example, comparing two of the investigated  $\text{TiO}_2$  materials by Hirakawa et al., that is, ST-21 (Ishihara, 100% anatase, BET surface area  $56.1 \text{ m}^2 \text{ g}^{-1}$ )<sup>30</sup> and PT101 (Ishihara, 100% rutile, BET surface area  $25 \text{ m}^2 \text{ g}^{-1}$ ),<sup>30</sup> one can clearly see that the formation rate of  $\text{OH}^\bullet$  radicals on ST-21, normalized to the BET surface area, is approximately 3 times higher than that on PT101. In our reported data, the formation rate of  $\text{OH}^\bullet$  radicals on the anatase (101) surface, normalized to the surface area, is  $\sim 2.8$  times higher than that on the rutile (110) surface. This good agreement between the ratio of the formation rates of  $\text{OH}^\bullet$  radicals on anatase and rutile powders and the ratio of the formation rates of  $\text{OH}^\bullet$  radicals on anatase (101) and rutile (110) surfaces can be explained by the fact that anatase (101) and rutile (110) are the thermodynamically most stable surfaces, and hence, anatase and rutile powders possess a large percentage of (101) and (110) surfaces, respectively. This might support the importance of the exposed surface on the photocatalytic activity and highlight the importance of investigating different well-defined surfaces and comparing the results with a nanomaterial exhibiting the corresponding exposed surface.

In conclusion, for the first time, the photocatalytic activities of a well-defined anatase  $\text{TiO}_2$  single-crystal (101) surface have experimentally been assessed by measuring the photocatalytic activity of methanol oxidation and by measuring the photocatalytic activity of  $\text{OH}^\bullet$  radical generation. Comparison of its photocatalytic activity with that of rutile  $\text{TiO}_2$  single-crystal (001), (100) and (110) surfaces indicates that the anatase (101) surface exhibits a higher activity than all investigated rutile surfaces toward methanol photo-oxidation and comparable  $\text{OH}^\bullet$  radical generation activity to that on the rutile (001) surface. The rutile (001) surface exhibits the highest photocatalytic activity among the three investigated rutile surfaces, while rutile (110) shows the lowest activity regardless of the employed test. Because the (101) and the (110) are the thermodynamically most stable surfaces for anatase and rutile, respectively,<sup>31–33</sup> it is expected that most synthesized anatase and rutile nanomaterials possess a large percentage of these surfaces. This explains why anatase usually exhibits a higher photocatalytic activity than rutile. The preparation of rutile nanomaterials with a large percentage of the (001) surface is expected to notably increase the photocatalytic activity of rutile nanomaterials.

## AUTHOR INFORMATION

### Corresponding Author

\*Tel.: +49-511-762-5560. E-mail: bahnmann@iftc.uni-hannover.de.

### Present Addresses

<sup>†</sup>Friemann & Wolf Batterietechnik GmbH, Industriestrasse 22, 63654 Büdingen, Germany.

## ACKNOWLEDGMENT

A.Y.A. thanks the Egyptian Ministry of Higher Education for providing her a doctoral scholarship (channel system) and the Chemistry Department, Faculty of Science, Sohag University, Egypt, for granting her a leave of absence. She also thanks Prof. J. Caro, Institute of Physical Chemistry and Electrochemistry, Leibniz University of Hannover, and Prof. F. Rashwan, Chemistry Department, Faculty of Science, Sohag University, for their support. We thank Mrs. V. Becker, Institute of Physical Chemistry and Electrochemistry, Leibniz University of Hannover, for the AFM measurements. The Financial support from the Bundesministerium für Bildung und Forschung (BMBF) is gratefully acknowledged (Grant No. 60420819).

## REFERENCES

- (1) Thompson, T. L.; Yates, J. T. Surface Science Studies of the Photoactivation of  $\text{TiO}_2$  — New Photochemical Processes. *Chem. Rev.* **2006**, *106*, 4428–4453.
- (2) Kavan, L.; Gratzel, M.; Gilbert, S. E.; Klemenz, C.; Scheel, H. J. Electrochemical and Photoelectrochemical Investigation of Single-Crystal Anatase. *J. Am. Chem. Soc.* **1996**, *118*, 6716–6723.
- (3) Prieto-Mahaney, O. O.; Murakami, N.; Abe, R.; Ohtani, B. Correlation between Photocatalytic Activities and Structural and Physical Properties of Titanium(IV) Oxide Powders. *Chem. Lett.* **2009**, *38*, 238–239.
- (4) He, Y. B.; Tilocca, A.; Dulub, O.; Selloni, A.; Diebold, U. Local Ordering and Electronic Signatures of Submonolayer Water on Anatase  $\text{TiO}_2(101)$ . *Nat. Mater.* **2009**, *8*, 585–589.
- (5) Amano, F.; Yasumoto, T.; Prieto-Mahaney, O. O.; Uchida, S.; Shibayama, T.; Ohtani, B. Photocatalytic Activity of Octahedral Single-Crystalline Mesoparticles of Anatase Titanium(IV) Oxide. *Chem. Commun.* **2009**, 2311–2313.
- (6) Tilocca, A.; Selloni, A. Methanol Adsorption and Reactivity on Clean and Hydroxylated Anatase(101) Surfaces. *J. Phys. Chem. B* **2004**, *108*, 19314–19319.
- (7) Mattioli, G.; Filippone, F.; Caminiti, R.; Bonapasta, A. A. Short Hydrogen Bonds at the Water/ $\text{TiO}_2$  (Anatase) Interface. *J. Phys. Chem. C* **2008**, *112*, 13579–13586.
- (8) Aschauer, U.; He, Y. B.; Cheng, H. Z.; Li, S. C.; Diebold, U.; Selloni, A. Influence of Subsurface Defects on the Surface Reactivity of  $\text{TiO}_2$ : Water on Anatase (101). *J. Phys. Chem. C* **2010**, *114*, 1278–1284.
- (9) Sanchez, V. M.; Cojulan, J. A.; Scherlis, D. A. Dissociation Free Energy Profiles for Water and Methanol on  $\text{TiO}_2$  Surfaces. *J. Phys. Chem. C* **2010**, *114*, 11522–11526.
- (10) Amano, F.; Prieto-Mahaney, O. O.; Terada, Y.; Yasumoto, T.; Shibayama, T.; Ohtani, B. Decahedral Single-Crystalline Particles of Anatase Titanium(IV) Oxide with High Photocatalytic Activity. *Chem. Mater.* **2009**, *21*, 2601–2603.
- (11) Sclafani, A.; Palmisano, L.; Schiavello, M. Influence of the Preparation Methods of  $\text{TiO}_2$  on the Photocatalytic Degradation of Phenol in Aqueous Dispersion. *J. Phys. Chem.* **1990**, *94*, 829–832.
- (12) Kominami, H.; Murakami, S.; Kato, J.; Kera, Y.; Ohtani, B. Correlation between Some Physical Properties of Titanium Dioxide Particles and Their Photocatalytic Activity for Some Probe Reactions in Aqueous Systems. *J. Phys. Chem. B* **2002**, *106*, 10501–10507.
- (13) Ohno, T.; Sarukawa, K.; Matsumura, M. Crystal Faces of Rutile and Anatase  $\text{TiO}_2$  Particles and Their Roles in Photocatalytic Reactions. *New J. Chem.* **2002**, *26*, 1167–1170.

- (14) Habibi, M. H.; Vosooghian, H. Photocatalytic Degradation of Some Organic Sulfides as Environmental Pollutants Using Titanium Dioxide Suspension. *J. Photochem. Photobiol., A* **2005**, *174*, 45–52.
- (15) Taguchi, T.; Saito, Y.; Sarukawa, K.; Ohno, T.; Matsumura, M. Formation of New Crystal Faces on TiO<sub>2</sub> Particles by Treatment with Aqueous HF Solution or Hot Sulfuric Acid. *New J. Chem.* **2003**, *27*, 1304–1306.
- (16) Zhang, Z. R.; Bondarchuk, O.; White, J. M.; Kay, B. D.; Dohnalek, Z. Imaging Adsorbate O–H Bond Cleavage: Methanol on TiO<sub>2</sub>(110). *J. Am. Chem. Soc.* **2006**, *128*, 4198–4199.
- (17) Wang, C. Y.; Groenzin, H.; Shultz, M. J. Direct Observation of Competitive Adsorption between Methanol and Water on TiO<sub>2</sub>: An in Situ Sum-Frequency Generation Study. *J. Am. Chem. Soc.* **2004**, *126*, 8094–8095.
- (18) Kandiel, T. A.; Dillert, R.; Bahnemann, D. W. Enhanced Photocatalytic Production of Molecular Hydrogen on TiO<sub>2</sub> Modified with Pt–Polypyrrole Nanocomposites. *Photochem. Photobiol. Sci.* **2009**, *8*, 683–690.
- (19) Kandiel, T. A.; Feldhoff, A.; Robben, L.; Dillert, R.; Bahnemann, D. W. Tailored Titanium Dioxide Nanomaterials: Anatase Nanoparticles and Brookite Nanorods as Highly Active Photocatalysts. *Chem. Mater.* **2010**, *22*, 2050–2060.
- (20) Jones, S. B.; Terry, C. M.; Lister, T. E.; Johnson, D. C. Determination of Submicromolar Concentrations of Formaldehyde by Liquid Chromatography. *Anal. Chem.* **1999**, *71*, 4030–4033.
- (21) Chen, J.; Ollis, D. F.; Rulkens, W. H.; Bruning, H. Photocatalyzed Oxidation of Alcohols and Organochlorides in the Presence of Native TiO<sub>2</sub> and Metallized TiO<sub>2</sub> Suspensions. Part (II): Photocatalytic Mechanisms. *Water Res.* **1999**, *33*, 669–676.
- (22) Wang, C. Y.; Rabani, J.; Bahnemann, D. W.; Dohrmann, J. K. Photonic Efficiency and Quantum Yield of Formaldehyde Formation from Methanol in the Presence of Various TiO<sub>2</sub> Photocatalysts. *J. Photochem. Photobiol., A* **2002**, *148*, 169–176.
- (23) Marugan, J.; Hufschmidt, D.; Lopez-Munoz, M. J.; Selzer, V.; Bahnemann, D. Photonic Efficiency for Methanol Photooxidation and Hydroxyl Radical Generation on Silica-Supported TiO<sub>2</sub> Photocatalysts. *Appl. Catal., B* **2006**, *62*, 201–207.
- (24) Sun, L. Z.; Bolton, J. R. Determination of the Quantum Yield for the Photochemical Generation of Hydroxyl Radicals in TiO<sub>2</sub> Suspensions. *J. Phys. Chem.* **1996**, *100*, 4127–4134.
- (25) Salinaro, A.; Emeline, A. V.; Zhao, J. C.; Hidaka, H.; Ryabchuk, V. K.; Serpone, N. Terminology, Relative Photonic Efficiencies and Quantum Yields in Heterogeneous Photocatalysis. Part II: Experimental Determination of Quantum Yields (Technical Report). *Pure Appl. Chem.* **1999**, *71*, 321–335.
- (26) Gao, R. M.; Stark, J.; Bahnemann, D. W.; Rabani, J. Quantum Yields of Hydroxyl Radicals in Illuminated TiO<sub>2</sub> Nanocrystallite Layers. *J. Photochem. Photobiol., A* **2002**, *148*, 387–391.
- (27) Fateh, R.; Ismail, A. A.; Dillert, R.; Bahnemann, D. W. Highly Active Crystalline Mesoporous TiO<sub>2</sub> Films Coated onto Polycarbonate Substrates for Self-Cleaning Applications. *J. Phys. Chem. C* **2011**, *115*, 10405–10411.
- (28) Ishibashi, K.; Fujishima, A.; Watanabe, T.; Hashimoto, K. Detection of Active Oxidative Species in TiO<sub>2</sub> Photocatalysis Using the Fluorescence Technique. *Electrochem. Commun.* **2000**, *2*, 207–210.
- (29) Hirakawa, T.; Yawata, K.; Nosaka, Y. Photocatalytic Reactivity for O<sup>•−</sup> and OH<sup>•</sup> Radical Formation in Anatase and Rutile TiO<sub>2</sub> Suspension as the Effect of H<sub>2</sub>O<sub>2</sub> Addition. *Appl. Catal., A* **2007**, *325*, 105–111.
- (30) Ohno, T.; Sarukawa, K.; Tokieda, K.; Matsumura, M. Morphology of a TiO<sub>2</sub> Photocatalyst (Degussa, P-25) Consisting of Anatase and Rutile Crystalline Phases. *J. Catal.* **2001**, *203*, 82–86.
- (31) Lazzeri, M.; Vittadini, A.; Selloni, A. Structure and Energetics of Stoichiometric TiO<sub>2</sub> Anatase Surfaces. *Phys. Rev. B* **2001**, *63*.
- (32) Diebold, U.; Ruzyski, N.; Herman, G. S.; Selloni, A. One Step Towards Bridging the Materials Gap: Surface Studies of TiO<sub>2</sub> Anatase. *Catal. Today* **2003**, *85*, 93–100.
- (33) Diebold, U. The Surface Science of Titanium Dioxide. *Surf. Sci. Rep.* **2003**, *48*, 53–229.